Polarization-Insensitive and Si Integrated Plug-and-Play MDI-QKD Transmitter

Kai-Wen Chen[1,2], Simone Atzeni[1,2], Dries Van Thourhout[1,2] and Stéphane Clemmen[1,2,3,4]

1. Photonics Research Group, INTEC Department, Ghent University-IMEC, 9052 Ghent, Belgium
2. Center for Nano- and Biophotonics (NB-Photonics), Ghent University, 9052 Ghent, Belgium
3. OPERA-Photonique CP 194/5, Université Libre de Bruxelles (ULB), 1000 Bruxelles, Belgium
4. Laboratoire d'Information Quantique CP224, Université Libre de Bruxelles, 1050 Bruxelles, Belgium

kaiwen.chen@ugent.be

***Abstract*—We demonstrate a polarization-insensitive MDI-QKD transmitter. The implementation of a 2D grating coupler enables the treatment of arbitrary input polarizations within a single TE-polarized circuit. We generate 400 MHz, 500 ps separated time-bin qubits with a QBER below 2%, ensuring high-speed integrated quantum communication.**

Keywords—Silicon photonics, Integrated transmitter, Quantum cryptography, plug-and-play MDI-QKD

I. Introduction

Measurement-Device-Independent QKD (MDI-QKD) provides robust security by eliminating detector side-channel attacks[1], yet its deployment is currently limited by the complexity of discrete fiber-optic hardware. Silicon Photonics offers a scalable, CMOS-compatible alternative [2]. However, a significant bottleneck remains: the high polarization sensitivity of silicon waveguides [3]. Standard silicon photonic components in a foundry process design kit (PDK) are typically designed for quasi-TE modes, necessitating active and precise polarization alignment of the incoming optical signal—a process that increases system complexity and requires power-hungry polarization controllers.

In this paper, we demonstrate a polarization-insensitive, integrated "Plug-and-Play" (P&P) MDI-QKD transmitter. By utilizing a bidirectional looped circuit with a 2D grating coupler (2DGC), we achieve polarization-insensitive operation that automatically compensates for fiber-induced polarization rotation. Operating at a 400 MHz clock rate with an average QBER of 2%, this transmitter enables low-cost, alignment-free nodes for robust, scalable quantum networks.

II. Design of Concept: Polarization-Insensitive Integrated P&P MDI-QKD Transmitter

The adopted P&P MDI-QKD protocol [4] is illustrated in Fig. 1(a). Charlie prepares phase-randomized weak coherent pulses (WCPs), which are split and transmitted to user nodes Alice and Bob via fibers. Users encode time-bin qubits using the photonic integrated circuit (PIC) and retro-reflect the pulses through the same fiber for Bell state measurement at Charlie.

The PIC architecture (Fig. 1(b)) utilizes a 2DGC to map orthogonal fiber polarizations to identical quasi-TE waveguide modes, propagating photons in clockwise (CW) or counterclockwise (CCW) direction based on the input state of

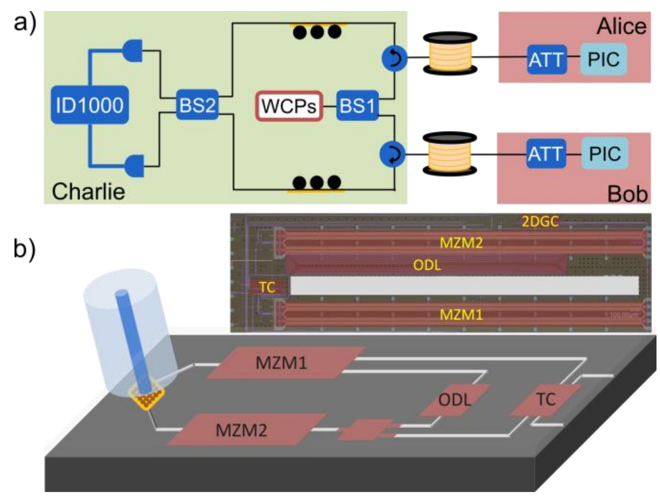

Fig. 1 (a) Experimental setup of P&P MDI-QKD scheme. (b) Schematic and microscope image of the PIC transmitter. ATT, attenuator.

polarization. In the CW path, an asymmetric Mach-Zehnder modulator (MZM1) routes light through either a short arm or through a long arm including a 500 ps optical delay line (ODL) to encode time-bin qubits, with an integrated thermally tunable coupler (TC) allowing to equalize arm losses. Subsequently, MZM2 performs intensity modulation to generate signal and decoy levels. Identical transformations in the CCW direction ensure polarization-independent operation across all encoding states, eliminating the need for active polarization alignment.

III. PIC Characterization

The 2DGC performance was evaluated using a 1D-2D test structure, injecting light via 1D grating couplers and out-coupling through the 2DGC. The transmission spectrum (Fig. 2(a)) reveals that the peak insertion losses of the 2DGC for both orthogonal polarization modes (s- and p-pol) are 6dB and shows that polarization-dependent loss (PDL) is observed between two modes across the spectrum. Fig. 2(b) shows the PDL versus coupling angle. PDL can be minimized at the laser operating wavelength by tuning the fiber coupling angle, thus ensuring the power balance required for stable MDI-QKD operation.

The thermal and electro-optic response of the active components was subsequently quantified. The TC features a P_π of 15mW with an extinction ratio (ER) above 30 dB (Fig. 2(c)). For the 5mm long MZMs, the measured half-wave voltage (V_π)

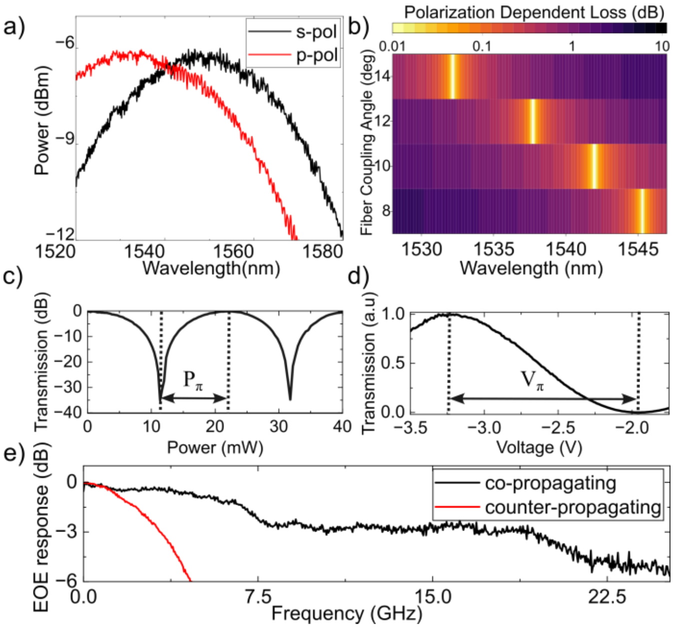

Fig.2 (a) 2DGC transmission spectrum . (b) PDL between s- and p-pol for several fiber coupling angles. (c) PIC heater half-wave power (Pπ). (d) PIC MZM half-wave voltage (Vπ). (e) PIC MZM high speed responses of co- and counter propagating signals.

was 1.4V (Fig. 2(d)), indicating high modulation efficiency. Electro-optic-electric (EOE) performance of the MZM was evaluated using a vector network analyzer (VNA). When the optical and RF signals are co-propagating, the MZM exhibits a 3-dB bandwidth exceeding 15 GHz (Fig. 2(e)). However, due to the looped P&P architecture, the optical signal travels in the opposite direction to the RF drive in one of the passes. In this counter-propagating configuration, the bandwidth is reduced to 1.5 GHz. Nevertheless, this remains significantly higher than the 400 MHz clock rate used in our time-bin qubit generation, thus ensuring negligible pulse distortion during high-speed encoding.

IV. Polarization Insensitive and Time-bin generation

The robustness of the integrated polarization-insensitive circuit was verified by sweeping the central paddle angle of a polarization controller from 0° to 160° to simulate fiber-induced polarization rotation and measured from the reflected pulse after the circulator. The peak pulse power remained remarkably stable (Fig. 3(a)), confirming that the 2DGC effectively maps arbitrary input states to the required quasi-TE mode, thereby eliminating the need for active feedback.

We implemented a time-bin MDI-QKD protocol to evaluate the transmitter's performance [4]. The heater and phase shifter of MZM1 were carefully set to prepare early or later time-bin states. The temporal profile of the generated states shown in Fig. 3(b) was characterized using a high-speed sampling oscilloscope (Tektronix DSA8300), where a pulse width of 121 ps at a 400 MHz repetition rate and high extinction ratio between early and late pulses were observed.

Quantum bit error rate (QBER) was obtained using a gated SPAD (5 MHz gate rate, 15% efficiency) and a time-tagger with 100ps resolution. By applying a 300 ps post-selection window to the coincidence histograms (Fig. 3(b)), we measured an average QBER of 2% across all time-bin states. This result sits

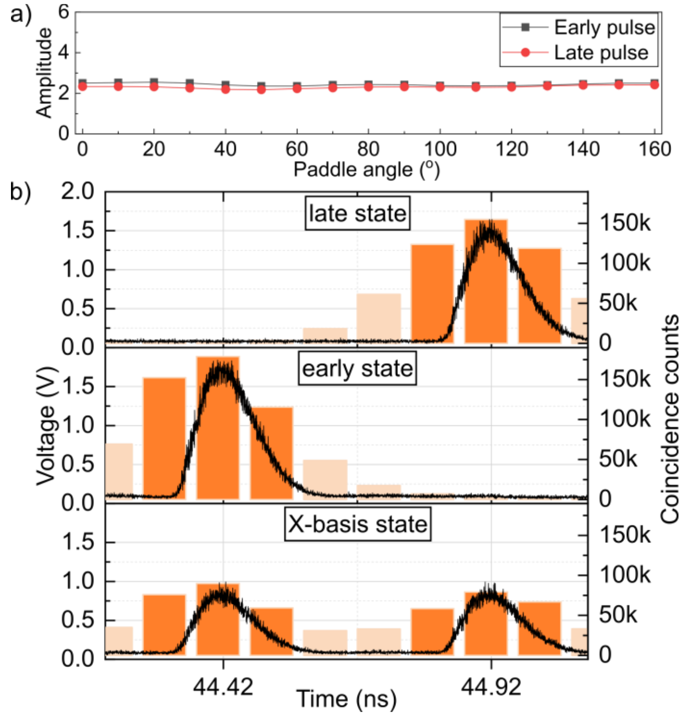

Fig.3 (a) Time-bin pulses amplitude variation with different polarization rotation. (b) Traces and histogram counts of PIC generated time-bin states.

well below the security threshold for MDI-QKD, validating the transmitter's readiness for integrated quantum networks.

Conclusion

We demonstrated a polarization-insensitive, silicon-integrated transmitter for plug-and-play MDI-QKD. A looped 2DGC configuration compensates for fiber-induced polarization drift, enabling the use of standard foundry PDK components and an operation free of any feedback loop. At a 400 MHz clock rate, the PIC achieved an average QBER of 2% and maintained stability across polarization rotation. By significantly reducing node complexity, this architecture provides a ready-to-use solution for QKD field deployment. Future work will focus on monolithic integration of sources and detectors to enhance quantum network scalability.

Acknowledgment

The authors thank funding by Digital-EU and Belspo through a QCI grant (Project 101091625 — Be-QCI) and Horizon Europe: Qu-Pilot (Grant agreement ID: 101113983). Stéphane Clemmen is a research associate of the FRS-FNRS.

References

[1] H.-K. Lo, M. Curty, and B. Qi, "Measurement-device-independent quantum key distribution," *Phys. Rev. Lett.*, vol. 108, no. 13, p. 130503, Mar. 2012.

[2] H. Semenenko, P. Sibson, A. Hart, M. G. Thompson, J. G. Rarity, and C. Erven, "Chip-based measurement-device-independent quantum key distribution," *Optica, OPTICA*, vol. 7, no. 3, pp. 238–242, Mar. 2020.

[3] D. Dai, L. Liu, S. Gao, D.-X. Xu, and S. He, "Polarization management for silicon photonic integrated circuits," *Laser & Photonics Reviews*, vol. 7, no. 3, pp. 303–328, 2013.

[4] F. Xu, "Measurement-device-independent quantum communication with an untrusted source," *Phys. Rev. A*, vol. 92, no. 1, p. 012333, Jul. 2015.